

Phase stability and elastic properties of $XMgB_{14}$ studied by *ab initio* calculations ($X=Al, Ge, Si, C, Mg, Sc, Ti, V, Zr, Nb, Ta, Hf$)

Helmut Kölpin,¹ Denis Music,¹ Graeme Henkelman,² and Jochen M. Schneider¹

¹Materials Chemistry, RWTH Aachen University, Kopernikusstrasse 16, D-52074 Aachen, Germany

²Department of Chemistry and Biochemistry, The University of Texas at Austin, Austin, Texas 78712-0165, USA

(Received 15 May 2008; revised manuscript received 1 August 2008; published 28 August 2008)

The effect of valence electron concentration (VEC) and size of the X element in $XMgB_{14}$ (space group *Imma* $X=Al, C, Si, Ge, Mg, Sc, Ti, V, Zr, Hf, Nb, Ta$) on stability and elastic properties was studied using *ab initio* calculations. Generally, icosahedral bonds, present in these compounds, are electron deficient. Based on the Bader charge analysis [Bader, *Atoms in Molecules: A Quantum Theory* (Oxford University Press, New York, 1990)] and density of states, X elements and Mg are shown here to transfer electrons to the boron network. Hence, the stability of the compounds studied increases as more electrons are transferred. As the VEC of the X element increases, fewer electrons are transferred to the boron network, and therefore the phase stability decreases. The bulk moduli of all compounds are in the range from 205 to 220 GPa. This can be understood analyzing the cohesive energy thereof. As the bulk modulus increases, the cohesive energy decreases.

DOI: 10.1103/PhysRevB.78.054122

PACS number(s): 62.20.D-, 71.20.Ps

I. INTRODUCTION

XMB_{14} compounds with the space group *Imma* exhibit interesting mechanical properties. Generally the X and M elements are metals in these borides. Their structure contains a complex boron framework based on icosahedral (B_{12}) boron units. Structure and stability of $AlMB_{14}$ based compounds were investigated experimentally for $M=Na, Li, Be, Mg, Ti, V, Cr, Mn, Fe, Co, Ni, Cu, Y, Tb, Dy, Ho, Er, Tm, Yb, Lu$.¹⁻⁸ The synthesis of the following stable bulk compounds was reported: $AlMgB_{14}$,^{1,2} $AlNaB_{14}$,⁴ $AlLiB_{14}$,⁵ and $AlMB_{14}$ ($M=Y, Tb, Dy, Ho, Er, Tm, Yb, Lu$).⁶⁻⁸ Furthermore, the substitution of Al in $AlMgB_{14}$ (Refs. 1 and 2) by Mg was communicated.⁹ Thin film synthesis of $AlMgB_{14}$ has also been attempted, but the as-deposited films were amorphous.¹⁰⁻¹²

Mechanical properties were studied for some of these compounds. Hardness values of 29–35 GPa (Refs. 13 and 14) for polycrystalline and 27–28 GPa (Ref. 3) for single-crystal $AlMgB_{14}$ were reported. The hardness of single crystalline $AlLiB_{14}$ was stated to be in the range between 24 and 29 GPa.³ Muthu *et al.*¹⁵ have recently reported a bulk modulus of 196 and 264 GPa for $AlMgB_{14}$ depending on the sample preparation. Moreover, calculations were carried out to characterize the elastic properties of $AlMgB_{14}$ based compounds. The calculated bulk moduli are in the range of 191–213 GPa for $AlMgB_{14}$ (Refs. 16 and 17) and 205 GPa for (Al, Si) MgB_{14} .¹⁶ In comparison, alumina, a well-known hard material, has a hardness value of 22 GPa and a bulk modulus of 246 GPa.¹⁸ B_6O is known to exhibit a hardness value of 35 GPa (Ref. 18) and its structure is based on icosahedral boron units. It was found that the hardness of $AlMgB_{14}$ can be increased by small additions of secondary phases.¹³ By the addition of TiB_2 hardness values of 40–46 GPa were reported,¹³ exceeding BN which is the second known hardest phase.¹⁸ Compared with diamond and cubic BN, $AlMgB_{14}$ possesses lower density, high chemical stability, and excellent electrical conductivity which makes it useful for numerous applications, such as cutting tools, hard and erosion-resistant coatings, wear resistant switch coat-

ings, and conductive thin films for microelectromechanical systems.¹⁹

The structural description for the XMB_{14} compounds is debated in the literature.^{1,2,4-6,9,20} Several structural proposals are available, differing in atomic positions, space group, and lattice-parameter designation. We use the description based on the latest refinement of $AlNaB_{14}$.⁴ Figure 1 shows this structure. An orthorhombic unit cell contains 64 atoms. Four boron icosahedra are located within the unit cell; there are eight boron sites between icosahedra and two other sites, $4b$ and $4e$, occupied by up to four X and M elements, respectively.⁴ For $AlMgB_{14}$, the X and M lattice sites are not fully occupied.¹ Higashi and Ito² reported a stoichiometry of $Al_{0.75}Mg_{0.78}B_{14}$. Almost the same occupancy ($Al_{0.75}Mg_{0.75}B_{14}$, 62 atoms) was used for the calculations of Lee and Harmon,¹⁷ where one Al and one Mg atom were missing at (0.5, 0.0, 0.0) and (0.5, 0.75, 0.391) sites, respectively. We use the latest refinement of $AlNaB_{14}$ (Ref. 4) combined with the occupancy proposal by Lee and Harmon¹⁷ for $X_{0.75}Mg_{0.75}B_{14}$, where the crystalline structure is unaffected upon vacancy formation.^{2,17} Even though XMB_{14} compounds have been studied extensively, there are no systematic studies of the influence of the X element se-

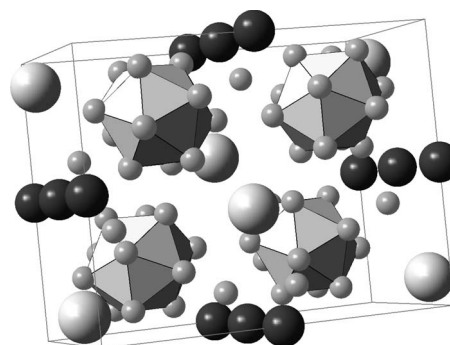


FIG. 1. Unit cell of the orthorhombic $AlMgB_{14}$ structure (space group: *Imma*), where small, dark, and bright spheres present B, Al, and Mg atoms, respectively.

lection on the electronic structure, the phase stability, and the elastic properties.

In this paper *ab initio* calculations are used to study the effect of valence electron concentration (VEC) and size of the X element in XMgB_{14} with 64 atoms and $X_{0.75}\text{Mg}_{0.75}\text{B}_{14}$ ($X=\text{Al, C, Si, Ge, Mg, Sc, Ti, V, Zr, Hf, Nb, Ta}$) with 62 atoms on stability and elastic properties. Two different occupancies were studied after Lee and Harmon.¹⁷ It is shown that stability of XMgB_{14} compounds is increased as more electrons are transferred to the boron icosahedra.

II. THEORETICAL METHODS

For the electronic structure calculations in this work, density-functional theory (DFT) (Ref. 21) was used. They were carried out using the generalized-gradient approximation^{22,23} and projector augmented wave potentials²⁴ with Blöchl corrections for the total energy.²⁵ These calculations were made in the Brillouin zone on a $5 \times 5 \times 5$ Monkhorst-Pack grid,²⁶ centered at the Γ point, within an energy cutoff of 500 eV and processed until the convergence criterion for the total energy of 0.01 meV was reached. The calculations were carried out at zero temperature and no pressure, applying an electron smearing of 0.2 eV based on the tetrahedron method with Blöchl corrections. The computer program used was the Vienna *ab initio* simulation package (VASP). For all calculations the internal free parameters (atomic positions) in a unit cell were relaxed first and then the lattice constants, i.e., a , b , and c (orthorhombic cell), were calculated. The calculated cohesive energies in this work are defined as negative values. The bulk modulus was obtained by subjecting the structure to uniform compression and tension up to 6% from the equilibrium volume and fitting the energy-volume curves to the Birch-Murnaghan equation of states.²⁷ The energy of formation was calculated with respect to pure elemental phases, which were obtained in the same manner as described above with the following space groups: $R\bar{3}m$ for $\alpha\text{-B}$, $P6_3/mmc$ for Mg, Hf, Sc, Ti, and Zr, $Fm\bar{3}m$ for Al, $Fd\bar{3}m$ for C, Si, and Ge, and $Im\bar{3}m$ for V, Ta, and Nb.

The chemical bonding was studied in terms of density of states as well as effective charge. The effective charge is referred to as a difference between the charge of a neutral atom and the total charge it possesses in a compound.²⁸ It was calculated by Bader charge analysis²⁹ applying the Bader analysis program developed by Henkelman and co-workers.^{30,31} Core charges were added to the charge-density distribution to verify the Bader regions.²⁹ In order to test precision, the fast Fourier transformation (FFT) grid was increased systematically for TaMgB_{14} . The default FFT grid for one unit cell was $108 \times 60 \times 84$. The deviation of the effective charge between the five and the six times finer FFT grid was less than 0.06%. All charges of XMgB_{14} were estimated on the base of six times finer FFT grid.

III. RESULTS AND DISCUSSION

Table I contains the calculated structural, phase stability, and mechanical property data for XMgB_{14} and

$X_{0.75}\text{Mg}_{0.75}\text{B}_{14}$, including available experimental data obtained by Higashi and Ito,² Muthu *et al.*,¹⁵ and Peters *et al.*²⁰ The lattice parameters are in a good agreement for $\text{Al}_{0.75}\text{Mg}_{0.75}\text{B}_{14}$ and MgMgB_{14} compared to the experimental data.^{2,18} The deviations are less than 0.2% and 0.6%, respectively. The phase stability is discussed in terms of the energy of formation (E_{form}). The most stable phase is ScMgB_{14} with $E_{\text{form}} = -0.180$ eV/atom. The calculated phases with $X=\text{C}$ and Ge are metastable. Comparing the two different occupancies, $X_{0.75}\text{Mg}_{0.75}\text{B}_{14}$ is more stable than XMgB_{14} for all studied X elements except of Mg and Sc. In literature, experimental data for the energy of formation of XMB_{14} are not available. To gain further understanding of the phase stability, the effective charge is calculated, as will be discussed below. $\text{Al}_{0.75}\text{Mg}_{0.75}\text{B}_{14}$ and AlMgB_{14} possess bulk moduli of 213 and 214 GPa, respectively. They are consistent with the theoretical values reported by Lowther¹⁶ of 208–213 GPa for AlMgB_{14} and by Lee and Harmon¹⁷ of 191 GPa for $\text{Al}_{0.75}\text{Mg}_{0.75}\text{B}_{14}$ and 212 GPa for AlMgB_{14} . Also the experimental values of the bulk modulus for AlMgB_{14} reported by Muthu *et al.*¹⁵ of 196 and 246 GPa are in agreement with the calculated values. The deviation of <20% lies within the expected range between theory and experiment.

The energy of formation, given in Table I, can be understood by studying the electronic structure. Since DFT derived density of states is not reliable in terms of empty states, we will not report on band-gap energies. Density of states is used here only to study general trends in the electronic structure. The total density of states (TDOS) for XMgB_{14} and $X_{0.75}\text{Mg}_{0.75}\text{B}_{14}$ for $X=\text{Mg, Al, Ti, V}$ is shown in Fig. 2. The more stable configurations with respect to occupancy are depicted by a solid line. It is apparent that the configuration with less states at the Fermi level is more stable. This is consistent with the results on AlMgB_{14} reported by Lee and Harmon.¹⁷ By introducing vacancies, i.e., forming $\text{Al}_{0.75}\text{Mg}_{0.75}\text{B}_{14}$, the total energy is lowered and the Fermi level falls below the band gap compared to AlMgB_{14} .¹⁷ In general, investigating the influence of the VEC on the electronic structure reveals that the band gap decreases as the VEC increases. While MgMgB_{14} has a pronounced band gap, there is only a pseudogap present for $\text{Ti}_{0.75}\text{Mg}_{0.75}\text{B}_{14}$ and $\text{V}_{0.75}\text{Mg}_{0.75}\text{B}_{14}$. This is probably of relevance regarding the properties; metallic behavior may be increased by the increase in the X element VEC. The band gap, in general, may originate from ionic bonding or hybridized states. However, the origin of the band gap is not known for XMgB_{14} compounds. To gain further understanding, the partial density of states (PDOS) of $\text{Al}_{0.75}\text{Mg}_{0.75}\text{B}_{14}$ was investigated, which is shown in Fig. 3. This enables the description of chemical bonding with respect to lattice sites as well as orbital quantum numbers. The TDOS is presented together with the PDOS of the corresponding s and p orbitals of Al, Mg, and two B atoms. One B atom, termed here as B_{ico} , is part of an icosahedron and a nearest neighbor of the other B atom, designated as B_{inter} , which is localized at an intermediate site between the B icosahedra. These Al and Mg atoms are both nearest neighbors of both B atoms but not of each other. The $\text{B}_{\text{inter}} p$ and $\text{B}_{\text{ico}} p$ orbitals overlap in the range from -10 to 0 eV and the strongest hybridization occurs from -3 to 0 eV. This indicates that they may be mainly

TABLE I. Calculated data for XMgB_{14} and $X_{0.75}\text{Mg}_{0.75}\text{B}_{14}$, including lattice parameters (a , b , and c), cohesive energy (E_{coh}), energy of formation (E_{form}), bulk modulus (B), effective charge per icosahedron ($q_{\text{eff ico}}$), and experimental lattice parameters and bulk modulus if applicable for $\text{Al}_{0.78}\text{Mg}_{0.75}\text{B}_{14}$ (Ref. 1), AlMgB_{14} (Ref. 15), and $\text{Mg}_{0.97}\text{Mg}_{0.97}\text{B}_{14}$ (Ref. 20) marked with *.

Phase	a (Å)	b (Å)	c (Å)	E_{coh} (eV/atom)	E_{form} (eV/atom)	B (GPa)	$q_{\text{eff ico}}$
AlMgB_{14}	10.378	5.895	8.154	-6.264	-0.092	214.0	-2.30
$\text{Al}_{0.75}\text{Mg}_{0.75}\text{B}_{14}$	10.308	5.838	8.113	-6.391	-0.103	213.0	-1.73
* $\text{Al}_{0.78}\text{Mg}_{0.75}\text{B}_{14}$	10.312(1)	5.848(1)	8.112(1)				
* AlMgB_{14}						196, 264	
CMgB_{14}	10.238	5.704	8.157	-6.271	0.241	215.0	-1.13
$\text{C}_{0.75}\text{Mg}_{0.75}\text{B}_{14}$	10.276	5.716	8.189	-6.383	0.168	208.0	-0.65
SiMgB_{14}	10.321	5.864	8.227	-6.247	0.034	209.0	-1.90
$\text{Si}_{0.75}\text{Mg}_{0.75}\text{B}_{14}$	10.292	5.817	8.132	-6.395	-0.023	212.0	-1.44
GeMgB_{14}	10.553	5.977	8.280	-6.122	0.101	201.0	-1.74
$\text{Ge}_{0.75}\text{Mg}_{0.75}\text{B}_{14}$	10.464	5.884	8.189	-6.285	0.042	205.0	-1.35
MgMgB_{14}	10.471	5.955	8.170	-6.172	-0.135	205.0	-2.15
* $\text{Mg}_{0.97}\text{Mg}_{0.97}\text{B}_{14}$	10.4809(5)	5.9738(3)	8.1255(4)				
$\text{Mg}_{0.75}\text{Mg}_{0.75}\text{B}_{14}$	10.438	5.920	8.152	-6.249	-0.066	201.0	-1.66
ScMgB_{14}	10.679	6.013	8.175	-6.515	-0.182	208.1	-2.17
$\text{Sc}_{0.75}\text{Mg}_{0.75}\text{B}_{14}$	10.493	5.973	8.167	-6.571	-0.159	205.8	-1.70
TiMgB_{14}	10.536	5.920	8.130	-6.599	-0.168	217.6	-2.07
$\text{Ti}_{0.75}\text{Mg}_{0.75}\text{B}_{14}$	10.350	5.895	8.107	-6.659	-0.170	216.0	-1.63
VMgB_{14}	10.422	5.866	8.106	-6.613	-0.120	224.1	-1.88
$\text{V}_{0.75}\text{Mg}_{0.75}\text{B}_{14}$	10.286	5.848	8.093	-6.662	-0.126	219.8	-1.47
ZrMgB_{14}	10.835	6.039	8.226	-6.586	-0.123	214.7	-2.28
$\text{Zr}_{0.75}\text{Mg}_{0.75}\text{B}_{14}$	10.595	5.998	8.180	-6.638	-0.124	211.7	-1.80
NbMgB_{14}	10.701	5.954	8.184	-6.659	-0.078	224.3	-2.09
$\text{Nb}_{0.75}\text{Mg}_{0.75}\text{B}_{14}$	10.522	5.850	8.139	-6.694	-0.090	219.4	-1.62
HfMgB_{14}	10.778	6.012	8.207	-6.682	-0.131	218.0	-2.30
$\text{Hf}_{0.75}\text{Mg}_{0.75}\text{B}_{14}$	10.550	5.978	8.162	-6.720	-0.139	214.3	-1.82
TaMgB_{14}	10.704	5.947	8.187	-6.736	-0.063	227.6	-2.12
$\text{Ta}_{0.75}\text{Mg}_{0.75}\text{B}_{14}$	10.503	5.923	8.139	-6.762	-0.087	222.4	-1.67

covalently bonded and that the bonding may be strong. For Al p there are less states below the Fermi level, which overlap to some extent with the B p orbitals. This can be seen in the region from -5 to -3 eV. Therefore, this hybridization is weaker. Mg does not seem to hybridize with its nearest neighbors. The Mg states below the Fermi level are almost empty and hence Mg exhibits negligible hybridization. These observations are consistent with the studies of the electron-density distribution by Lowther.¹⁶ Investigating the states around the Fermi level shows that the bonding and antibonding states are separated by the band gap or by the pseudogap (see Fig. 2). Therefore, the orbitals overlap symmetrically, which implies, according to Gelatt *et al.*,³² that this configuration should be more stable than others where antibonding states are filled or partially filled. AlMgB_{14} with a band gap below the Fermi level is less stable than $\text{Al}_{0.75}\text{Mg}_{0.75}\text{B}_{14}$ with the band gap at the Fermi level.

Since the Mg orbitals do not give rise to hybridized states, ionic contributions to the overall bonding may be important and required to explain the phase stability. To gain further

understanding of the role of the X element and Mg on stability of XMgB_{14} , the effective charge was studied by Bader charge analysis.²⁹ The phase stability of these borides may be dependent on the charge transfer to the boron framework. Longuet-Higgins and Roberts³³ reported that B icosahedra are electron deficient and need two additional electrons to be stabilized. Therefore, it is required to study the correlation between the effective charge of icosahedra and stability as a function of VEC and size of the X elements. The effective charge of icosahedra in the investigated XMgB_{14} compounds, related to the more stable configuration with respect to $4a$ and $4b$ site occupancies, ranges from -0.65 to -2.17 (see Table I). While in the X elements effective charge varies between -1.07 and $+2.34$ and the B_{inter} atoms between -0.65 and $+0.09$, the effective charge of Mg in all XMgB_{14} compounds studied varies between $+1.65$ and $+1.70$, suggesting that Mg is ionically bonded. Figure 4 shows the effective charge per icosahedron for the more stable configuration with respect to occupancy (empty squares: $X_{0.75}\text{Mg}_{0.75}\text{B}_{14}$; crossed squares: XMgB_{14}) as a function of Pauling's elec-

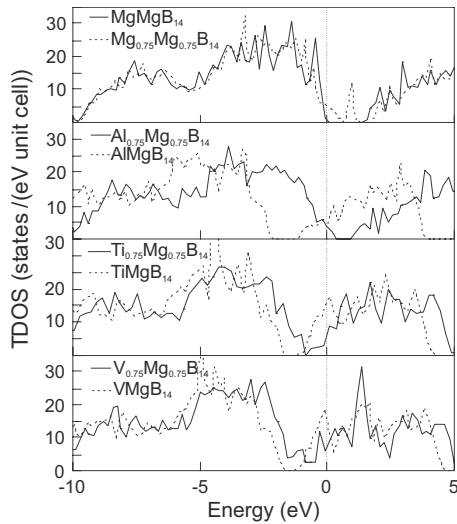


FIG. 2. TDOS of $XMgB_{14}$ ($X=Mg, Al, Ti, V$) for two cases each: fully occupied $XMgB_{14}$ and $X_{0.75}Mg_{0.75}B_{14}$. The solid lines designate the TDOS of more stable configurations with respect to occupancy. The Fermi energy is set to 0 eV.

tronegativity. The effective charge of icosahedra is more positive for X elements with larger electronegativity. Because of this dependency, the changes in the effective charge may indicate that X elements in $XMgB_{14}$ are also ionically bonded, which is consistent with the observations based on the PDOS, as discussed above. This enables investigation on how the effective charge of icosahedra influences the stability of the $XMgB_{14}$ compounds. Figure 5 shows the energy of formation as a function of the effective charge of a B icosahedron. The more stable configuration with respect to occupancy is shown for every $XMgB_{14}$ compound (filled square:

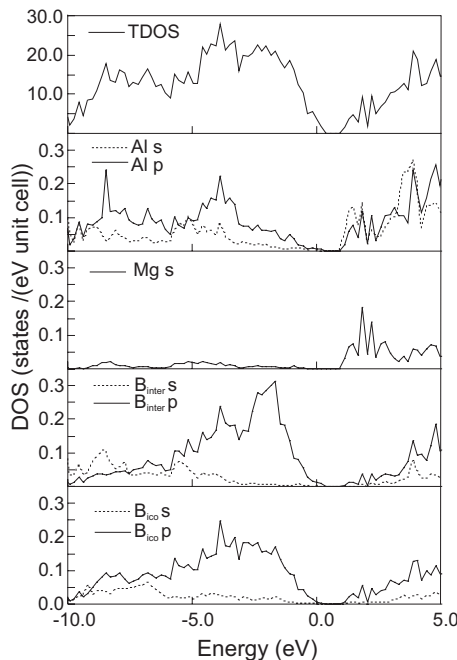


FIG. 3. PDOS of $Al_{0.75}Mg_{0.75}B_{14}$ for single Al, Mg, B_{inter} , and B_{ico} atoms, as well as TDOS. The Fermi energy is set to 0 eV.

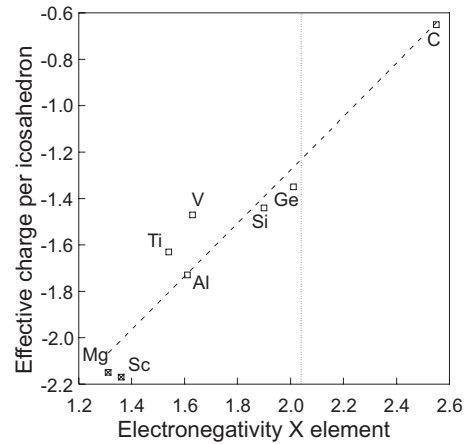


FIG. 4. Effective charge per icosahedron as a function of electronegativity for the more stable configuration with respect to occupancy. $X_{0.75}Mg_{0.75}B_{14}$ or $XMgB_{14}$ are represented by empty and crossed squares, respectively. The electronegativity of B is shown as a reference by the dotted vertical line.

$XMgB_{14}$; half filled square: $X_{0.75}Mg_{0.75}B_{14}$). The $XMgB_{14}$ compounds with the VEC changes induced by s, p (Mg, Al, Si), and d (Sc, Ti, V) states of X elements are linked by a solid line. A dashed line is used to connect $XMgB_{14}$ compounds with X atoms of different sizes. As the VEC of the X element increases from 0 to 2 p valence electrons (Mg, Al, Si) and from 1 to 3 d valence electrons (Sc, Ti, V), the effective charge of an icosahedron increases from -2.15 to -1.44 and from -2.17 to 1.47 , respectively. This is consistent with the increasing electronegativity of the X elements with a larger VEC. The critical electronegativity of the X element in $XMgB_{14}$ is between 1.90 and 2.01. Therefore, in the compounds containing X elements with a larger VEC fewer electrons are transferred to the boron network and the energy of formation increases from -0.135 to -0.023 eV/atom (Mg, Al, Si) and -0.182 to -0.126 eV/atom (Sc, Ti, V) so that the phase stability decreases. The most stable $XMgB_{14}$ com-

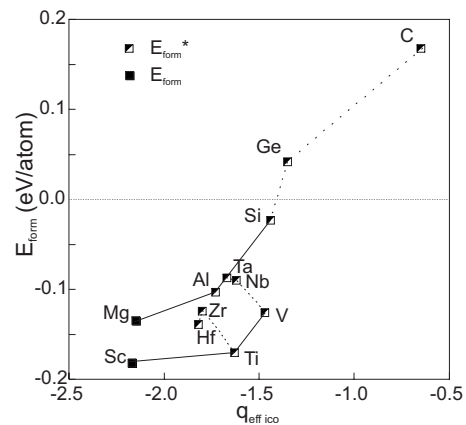


FIG. 5. Energy of formation (E_{form}) for the more stable configuration with respect to occupancy (either $XMgB_{14}$ or $X_{0.75}Mg_{0.75}B_{14}$ marked with *) vs the effective charge of icosahedra ($q_{eff\ ico}$). $XMgB_{14}$ compounds with a different VEC induced by s, p (Mg, Al, Si) and d (Sc, Ti, V) states of X elements are linked by a solid line, while X atoms of different sizes are linked with a dashed line.

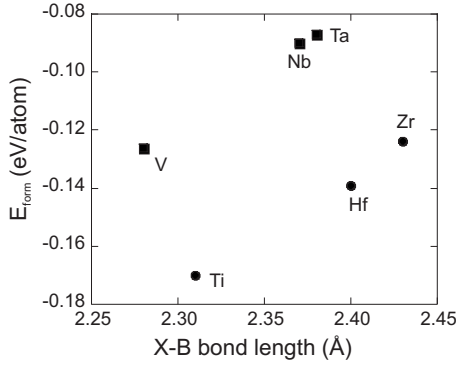


FIG. 6. Energy of formation (E_{form}) for the $X_{0.75}\text{Mg}_{0.75}\text{B}_{14}$ configuration ($X=\text{Ti}, \text{Zr}, \text{Hf}, \text{V}, \text{Nb}, \text{Ta}$) with respect to the average X-B bond length.

pounds are ScMgB_{14} and $\text{Ti}_{0.75}\text{Mg}_{0.75}\text{B}_{14}$. $\text{Si}_{0.75}\text{Mg}_{0.75}\text{B}_{14}$ is still stable, while $\text{Ge}_{0.75}\text{Mg}_{0.75}\text{B}_{14}$ and $\text{C}_{0.75}\text{Mg}_{0.75}\text{B}_{14}$ are not. In the case of C as the X element, its role in XMgB_{14} seems to be of different nature as compared, for example, with B_4C structures.³⁴ X elements and Mg in XMgB_{14} transfer electrons to the B network, while C forms cross-linking C-B-C chains in B_4C .³⁴ It is energetically favorable for C to covalently cross-link with B instead of forming metallic or ionic bonds. To study the size effect of the X element on the stability of XMgB_{14} , we investigate the average bond length between the X element and its nearest 12 B neighbors (average X-B bond length). Guette *et al.*⁹ used the average X-B bond length as an indicator for the hole size in the lattice and reported an average X-B bond length in Mg_2B_{14} of 2.33 Å. For $\text{Al}_{0.75}(\text{Mg}_{0.5}\text{Al}_{0.25})\text{B}_{14}$ based on the results of Matkovich and Economy,¹ an average X-B bond length of 2.27 Å (Ref. 9) was estimated. In this work, we obtain the average X-B bond length for Mg_2B_{14} and $\text{Al}_{0.75}\text{Mg}_{0.75}\text{B}_{14}$ of 2.34 and 2.28 Å, respectively. These values are consistent with the experimental results.⁹ Figure 6 shows the energy of formation as a function of the average X-B bond length for $X_{0.75}\text{Mg}_{0.75}\text{B}_{14}$ with $X=\text{IVB}$ (Ti, Zr, Hf) and VB (V, Nb, Ta). The energy of formation increases linearly with increasing X-B bond length. This may indicate that XMgB_{14} phases with smaller X elements are more stable, which is consistent with the notion introduced by Guette *et al.*,⁹ as discussed above. We speculate that the larger X elements deform the boron framework and therefore may strain the lattice. This may cause a decrease in the phase stability observed here. The dashed lines in Fig. 5 also show the increase in the energy of formation introduced by the size of the different X elements.

The bulk modulus values obtained (see Table I) can be understood studying the cohesive energy. All studied compounds have bulk moduli in the range of 205–220 GPa. Figure 7 shows the cohesive energy and the bulk modulus for XMgB_{14} as a function of VEC. The X elements with 1 and 2 p electrons are Al and Si, while Sc, Ti, and V possess 1, 2,

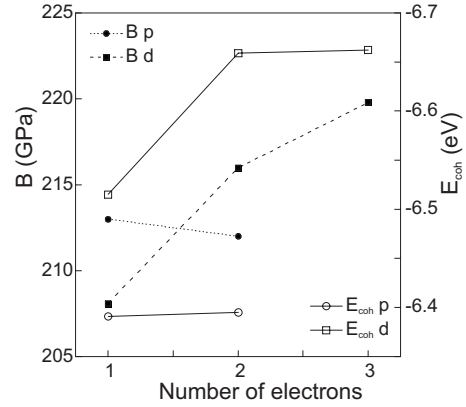


FIG. 7. Bulk modulus (B) and cohesive energy (E_{coh}) of XMgB_{14} for different VEC (p and d).

and 3d electrons, respectively. Also, in this figure the more stable configurations with respect to occupancy are considered. With a decrease in the cohesive energy from -6.515 to -6.662 eV/atom, the bulk modulus is increasing from 208 to 220 GPa for Sc, Ti, and V. For the compounds containing Al or Si, no significant change in the cohesive energy (-6.391 and -6.395 eV/atom) and the bulk modulus (213 and 212 GPa) is observed. This behavior is expected because stronger bonds are found in the compound with a lower cohesive energy. Different X elements do not induce significant changes in the bulk modulus. This indicates that the main contribution to the bulk modulus is given by the boron framework. The X elements transfer charge to the boron framework and therefore affect the phase stability, but they do not seem to form strong bonds with the boron framework.

IV. CONCLUSION

We have studied the effect of the VEC and the size of the X element ($X=\text{Al}, \text{C}, \text{Si}, \text{Ge}, \text{Mg}, \text{Sc}, \text{Ti}, \text{V}, \text{Zr}, \text{Hf}, \text{Nb}, \text{Ta}$) on the phase stability and the elastic properties of XMgB_{14} and $X_{0.75}\text{Mg}_{0.75}\text{B}_{14}$ compounds using *ab initio* calculations. All $X_{0.75}\text{Mg}_{0.75}\text{B}_{14}$ phases are more stable than XMgB_{14} except for the configurations with $X=\text{Mg}$ or Sc. As revealed by the PDOS analysis, this may be related to the filling of the antibonding states in XMgB_{14} . Generally, icosahedral bonds, present in these compounds, are electron deficient. Based on the Bader charge analysis²⁹ and PDOS, as well as TDOS, X elements and Mg transfer electrons to the boron network. Hence, the stability of the compounds studied increases as more electrons are transferred. As the VEC of the X element increases, fewer electrons are transferred to the boron network, and therefore the phase stability decreases. The bulk moduli of all compounds are in the range from 205 to 220 GPa. This can be understood analyzing the cohesive energy thereof. As the bulk modulus increases, the cohesive energy decreases.

- ¹V. I. Matkovich and J. Economy, *Acta Crystallogr., Sect. B: Struct. Crystallogr. Cryst. Chem.* **26**, 616 (1970).
- ²I. Higashi and T. Ito, *J. Less-Common Met.* **92**, 239 (1983).
- ³I. Higashi, M. Kobayashi, S. Okada, K. Hamano, and T. Lundstroem, *J. Cryst. Growth* **128**, 1113 (1993).
- ⁴S. Okada, T. Tanaka, A. Sato, T. Shishido, K. Kudou, K. Nakajima, and T. Lundstroem, *J. Alloys Compd.* **395**, 231 (2005).
- ⁵I. Higashi, *J. Less-Common Met.* **82**, 317 (1981).
- ⁶M. M. Korsukova, T. Lundstroem, L. E. Terenius, and V. N. Gurin, *J. Alloys Compd.* **187**, 39 (1992).
- ⁷M. M. Korsukova, V. N. Gurin, Y. B. Kuz'ma, N. F. Chaban, S. I. Chykhrii, V. V. Moshchalkov, N. B. Brandt, A. A. Gippius, and H. N. Ho, *Phys. Status Solidi A* **114**, 265 (1989).
- ⁸M. M. Korsukova, V. N. Gurin, Y. Yu, L. E. Terenius, and T. Lundstroem, *J. Alloys Compd.* **190**, 185 (1993).
- ⁹A. Guette, M. Barret, R. Naslain, P. Hagenmuller, L. E. Terenius, and T. Lundstroem, *J. Less-Common Met.* **82**, 325 (1981).
- ¹⁰Y. Tian, M. Womack, P. Molian, C. C. H. Lo, J. W. Andereg, and A. M. Russell, *Thin Solid Films* **418**, 129 (2002).
- ¹¹Y. Tian, A. Constant, C. C. H. Lo, J. W. Andereg, A. M. Russell, J. E. Snyder, and P. Molian, *J. Vac. Sci. Technol. A* **21**, 1055 (2003).
- ¹²M. Stock and P. Molian, *J. Vac. Sci. Technol. A* **22**, 670 (2004).
- ¹³B. A. Cook, J. L. Haringa, T. L. Lewis, and A. M. Russell, *Scr. Mater.* **42**, 597 (2000).
- ¹⁴V. Kevorkijan, S. D. Skapin, M. Jelen, K. Krnel, and A. Meden, *J. Eur. Ceram. Soc.* **27**, 493 (2007).
- ¹⁵D. V. S. Muthu, B. Chen, B. A. Cook, and M. B. Kruger, *High Press. Res.* **28**, 63 (2008).
- ¹⁶J. E. Lowther, *Physica B (Amsterdam)* **322**, 173 (2002).
- ¹⁷Y. Lee and B. N. Harmon, *J. Alloys Compd.* **338**, 242 (2002).
- ¹⁸D. M. Teter, *MRS Bull.* **23**, 22 (1998).
- ¹⁹R. Cherukuri, M. Womack, P. Molian, A. Russel, and Y. Tian, *Surf. Coat. Technol.* **155**, 112 (2002).
- ²⁰J. S. Peters, J. M. Hill, and A. M. Russell, *Scr. Mater.* **54**, 813 (2006).
- ²¹P. Hohenberg and W. Kohn, *Phys. Rev.* **136**, B864 (1964).
- ²²J. P. Perdew, in *Electronic Structure of Solids '91*, edited by P. Ziesche and H. Eschrig (Akademie, Berlin, Germany, 1991), p. 11.
- ²³J. P. Perdew and Y. Wang, *Phys. Rev. B* **45**, 13244 (1992).
- ²⁴G. Kresse and D. Joubert, *Phys. Rev. B* **59**, 1758 (1999).
- ²⁵P. E. Blochl, *Phys. Rev. B* **50**, 17953 (1994).
- ²⁶H. J. Monkhorst and J. D. Pack, *Phys. Rev. B* **13**, 5188 (1976).
- ²⁷F. Birch, *J. Geophys. Res.* **83**, 1257 (1978).
- ²⁸A. L. Allred and E. G. Rochow, *J. Inorg. Nucl. Chem.* **5**, 264 (1958).
- ²⁹R. Bader, *Atoms in Molecules: A Quantum Theory* (Oxford University Press, New York, 1990).
- ³⁰G. Henkelman, A. Arnaldsson, and H. Jónsson, *Comput. Mater. Sci.* **36**, 354 (2006).
- ³¹E. Sanville, S. D. Kenny, R. Smith, and G. Henkelman, *J. Comput. Chem.* **28**, 899 (2007).
- ³²C. D. J. Gelatt, A. R. Williams, and V. L. Moruzzi, *Phys. Rev. B* **27**, 2005 (1983).
- ³³H. C. Longuet-Higgins and M. de V. Roberts, *Proc. R. Soc. London* **230**, 110 (1955).
- ³⁴R. Lazzari, N. Vast, J. M. Besson, S. Baroni, and A. Dal Corso, *Phys. Rev. Lett.* **83**, 3230 (1999).